AN EXPERIMENTAL STUDY ON VIBRATIONAL CHARACTERISTICS OF WALL FOUNDATION PILE

K. Wakamatsu (I)

SUMMARY

Dynamic experiments concerning deformations ranging from microsopic to massive were conducted on cast-in-place reinforced concrete piles of rectangular cross section and possessing directionality in behaviors in the horizontal direction, and these and results of examinations of the experiments are described. As a result of the experiments it is recognized that the dynamic characteristics vary greatly depending on the degree of stiffness of the pile and differences in the natures of subgrade reactions. It is shown that skeleton curves and characteristic hysteresis loops at times of massive deformations can be satisfactorily explained by a simple analysis model considering separation between pile and soil along with nonlinearities of pile and soil.

INTRODUCTION

The Wall-Foundation Pile (hereafter called WF Pile) which was the object of this study is a cast-in-lace reinforced concrete pile constructed by the OWS-SOLETANCHE Method. The feature of this pile is that because the cross section is rectangular, there is a directionality to the dynamic characteristics in the horizontal direction, and different behaviors are demonstrated beween the in-plane (strong-axis) direction and out-of-plane (weak-axis) direction.

In general, since outdoor vibration generator experiments of piles mostly use actual piles as objects, it is difficult for experiments up to the extent of massive deformations to be carried out when vibration generator capacity is considered, and there are hardly any such cases seen. The purposes of the present study are to experimentally grasp the vibrational characteristics of WF Piles in the range of microscopic to massive deformations, obtain fundamental data concerning dynamic analyses, and utilize these for establishment of a more rational design technique for this type of pile.

OUTLINE OF EXPERIEMNTS

Test Ground

The ground in a natural state is composed of fill, loam deposit, and gravel deposit in order from the top. The test ground, as shown in Fig. 1, was a plane area of approximately 8 m x 8 m excavated to a depth of 1 m, with the surface fill removed to expose loam producing a simple ground of a two-layered system. S-wave velocities measured at the surface of the test ground were approximately 100 to 120 m/sec. The results of various laboratory tests on soil samples collected at the site are shown in Fig. 2. Judged by this figure, it is thought that S-wave velocities obtained on the excavated surface indicate slightly low values, and it is considered this is the influence

(I) Research Engineer, Technical Research Institute, OHBAYASHI-GUMI, Ltd., Tokyo, Japan

of stress relief due to excavation. Internal damping by the ground is about 3% at the microscopic deformation level. The density of loam was approximately 1.3 t/m^3.

Test Pile

The model WF Piles were cast-in-place piles made by dry excavation of rectangular pile shapes in the ground, inserting reinforcing bar cage assemblies, and placing mortar inside. The test piles, as shown in Fig. 1, were the three of A, B, C, the pile lengths all being 4.9 m and pile ends reaching a gravel layer. The cross-sectional shapes were 720 mm x 120 mm for Piles A and B, and 360 mm x 120 mm for Pile C. The reinforcing bar arrangements of the piles are shown in Fig. 3. The directions of vibration were in-plane for Piles A and C, and out-of-plane for Pile B. A footing for a vibration generator was provided at the head of each pile, and for the sake of simplification of the analysis model, the bottom surface of the footing was isolated from the surface of the ground. The stress-strain relationship of the reinforcing steel and mortar used is shown in Fig. 4.

Measurement Items

Measurement items were displacement of footing, acceleration at footing, acceleration in pile, axial strain of main reinforcement, and acceleration in surrounding ground. The previously-mentioned Fig. 1 shows only the locations of the accelerometers installed in the pile bodies.

Vibration Generator and Method of Experimentation

The vibration generator was a horizontally-rotating unbalanced-weight type, with maximum exciting force of 3 tons, and excitation frequency range 0.2 - 20 c/s. The total weight in a condition of the vibration generator installed on the footing was approximately 4 tons. The case of Pile C is given in Table 1 as an example of the experimentation procedure. As shown in this table, the experiments consisted of combinations of continuous excitation experiments (RUN) and stepped experiments (STEP) at the microscopic deformation level. The RUN experiments consisted of determining the final excitation frequency based on natural frequency at a low level measured beforehand, and causing massive deformation in the pile in a condition of resonance by continuously raising the number of revolutions of the vibration generator up to that frequency. The numbers of cycles in the virgin deformation ranges during individual RUN experiments were about 3 to 5 times with Pile B and C, but in the case of Pile A, because natural frequency was high, the number of repetitions was fairly large. As for STEP experiments, they were conducted before and after the RUN experiments, and the transitions of vibration characteristics at microscopic deformation levels were discerned. An example of the recorded waveforms is shown in Fig. 5.

RESULTS OF EXPERIMENTS

Dynamic Hysteresis Loops

The dynamic hysteresis loops of each soil-pile system were obtained using the horizontal external force obtained considering the exciting force of the vibration generator in addition to inertia force at the centroid of the foot-

ing and vibration generator and the horizontal displacement obtained at the side surface of the footing. The hysteresis loops of piles at comparatively small deformations and massive deformations in RUN experiments are shown in Figs. 6 and 7. These hysteresis loops differ in numbers of cycles and effects of damping with the individual piles, but roughly, they can be analyzed as follows.

As shown in Fig. 6, at a level of comparatively small deformations, all of the piles show hysteresis forms which are approximately spindle-shaped, and the piles and soil are thought to exhibit elastic behaviors. However, the shapes at the level of massive deformations are characteristically different as shown in Fig. 7. In a case such as Pile A where pile stiffness in the in-plane direction is great and deformation of the pile extends down to deep parts of the pile for a short pile effect, and in addition the subgrade reaction is predominantly due to shearing at side surfaces of the pile, hysteresis loops are of spindle shapes.

In contrast, as with Pile C, even though in the same in-plane direction, with stiffness comparatively weak and massive deformation occurring near the ground surface for a long pile effect where it may be considered that the ratio of the subgrade reaction due to compression at the front of the pile is high, hysteresis loops constricted in the vicinity of the origin are indicated. This is thought to be because gaps are formed near the ground surface between the pile and the soil at the front and back of the pile as the amount of deformation increases, and moreover, the subgrade reaction at the side loses effect, and restoring force near the origin is reduced. Such a trend can be recognized with Pile B also.

Damping

Equivalent viscous damping was calculated from the areal ratios of the hystresis loops in states of almost reasonance, comparisons were made with resonance frequencies, and these are shown in Fig. 8. The damping coefficients obtained from the STEP experiments are also shown. The equivalent viscous damping obtained from hysteresis loops is thought to be affected by the incremental pitch during excitation and the excitation history, and although it is difficult to evaluate the piles at the same level, all of the piles show trends of increase together with deformation quantities (drop of resonance frequencies), and at the massive deformations, values about 1.5 to 3 times those at microscopic deformations are indicated. As for damping at times of microscopic deformations obtained from the individual STEP experiments, there is a trend for slight decrease while the deformation experienced is not very great, but a trend of increase is shown when deformation becomes large. This is thought to be because a trend of decrease is indicated due to the effect of gaps between soil and pile, but from a level at which it may be considered that a fair amount of damage has occurred in this pile itself, the effect becomes great.

The primary natural frequency of the test ground is also given in this figure. According to M, Novak, regarding a pile having a natural frequency lower than the primary natural frequency of the ground, radiation damping is small (Ref. 1), and it is thought that internal damping and hysteretic damping of piles and soil are governing factors in damping of Piles B and C. The damping quantities of Piles B and C at the microscopic deformation level are

around 4 to 5% and comparatively close to the results of soil tests, but with Pile A of high resonance frequency a value of about 10% is indicated and substantial radiation damping is inferred.

DISCUSSION

Skeleton Curve and Deformation Distribution of Pile

The soil-pile system was discretized and modelled as shown in Fig. 9, and the skeleton curve was examined on causing shear force and moment estimated from the experiments to statically act at the pile head. Causing to act statically is strictly an approximate measure, but is thought to pose no problem in grasping the overall characteristics macroscopically. The stiffnesses of the pile and soil were evaluated as described below. The initial stiffness of the pile was evaluated by the beam theory considering bending and shearing deformation, while the relation between bending moment and curvature in the nonlinear range was modelled trilinearly using the stress-strain relation shown in Fig. 4, and obtaining the bending moments and curvatures at cracking, yielding of outermost reinforcing bar, and ultimate failure, respectively. With regard to sharing, elasticity was maintained. As for subgrade reaction, evaluation was done by determining the force required when a unit displacement was provided an arbitrary layer based on Mindlin's solution (Ref. 2). Regarding the displacement dependence of subgrade reaction, the value obtained by the equation proposed by K. Kotoda, S. Kazama et al. (Ref. 3) simplified into trilinear form as shown in Fig. 10 was used.

The hysteresis loops at the massive deformations on Piles A, B, and C and the skeleton curves obtained by calculations are shown in the previously-mentioned Fig. 7. In the figure, the broken line is for a case when subgrade reaction acted effectively over the entire range of deformation, while the dot-dash line is for the case when it was assumed there would be loss of effectivenss if the subgrade reactions acting at the side surfaces of the pile were to become greater than the shearing strength of soil. The shearing strength of soil was taken to be 1/2 of the unconfined compressive strength obtained in soil tests. As for the rate of subgrade reactions acting on the front and sides of the pile, it was assumed that the ratio when elastic would be maintained unaltered. The relations of equivalent stiffness determined from resonance frequency and deformation at footing are compared in Fig. 11. The calculated values are also shown and these values are those indicated by the dot-dash line in Fig. 7. According to these figures, the experimental and calculated values of Piles B and C agree comparatively well, and by considering the nonlinearities of pile and soil, and loss of subgrade reactions at side surfaces of the pile, the experimental results are aptly explained. With respect to Pile A, a trend is indicated of calculated value exceeding experimental value in the range of large deformation. This is thought to have been because subgrade reactions at the side surfaces of the pile expired at a low stress level due to the effect of repetitions. Further, according to Fig. 11, with Piles B and C, the equivalent stiffnesses obtained from RUN experiments were smaller than those obtained from STEP experiments while deformations were small to indicate trends of so-called soft-spring type, but when the deformations became larger there was a slight transition to hard-spring type and reduction in stiffnesses of piles and increase in gaps between piles and soil were seen.

The normalized deformation distributions are shown in Fig. 12. Since normalized deformation distributions did not vary graatly according to level of displacement, those for the elastic range are shown. The experimental and calculated values indicate comparatively good correspondence, and the stiffness evaluations of the piles and ground are considered to have been appropiate.

Simulation of Hysteresis Loops

An attempt was made to express characteristic hysteresis loops by simple models. Simulation analyses were performed independently setting up characteristics of subgrade reactions acting on the pile, the front and back surfaces of the pile, and the side surfaces of the pile. The restoring force characteristics set up are shown in Fig. 13. Since there were no cases in the present study of reinforcing bars far exceeding yield points, the piles were taken to be origin-oriented types, while concerning subgrade reactions acting on the front and back surfaces of piles, double bilinear types considering separation of piles and soil were taken. As for soil at the side surfaces of piles, the hysteresis loops are spindle-shaped such as seen for hollow torsional dynamic triaxial tests. The hysteresis loops of Piles B and C calculated for massive deformations, where radiation damping was small and hysteretic damping was considered to be governing, are shown in Fig. 14 compared with experimental results. Since the hysteresis loops obtained from experiments contain the influences of damping terms in the restoring force terms, in a strict sense comparisons cannot be made, but the two correspond relatively well with each other, and it is thought characteristic hysteresis loops are aptly expressed.

CONCLUSION

As a result of the experiments, it was found that pile stiffness and the properties of subgrade reaction have great influences on the behaviors of a pile in in-plane and out-of-plane directions. It was also found that the behaviors of skelteton curves and characteristic hysteresis loop could be explained well by a simple method of separately evaluating the subgrade reactions acting on the pile, the front and back surfaces of the pile, and the side surfaces of the pile.

ACKNOWLEDGEMENTS

The author sincerely thanks Dr. Kyoji Nakagawa, former Director, and Mr. Seiji Watanabe, Laboratory Chief, of OHBAYASHI-GUMI Technical Research Institute for their guidance in carrying out the study, and Mr. Fumio Chatani, Research Engineer, Soil Mechanics and Foundation Engineering Laboratory, for his valuable advice in various aspects of the work.

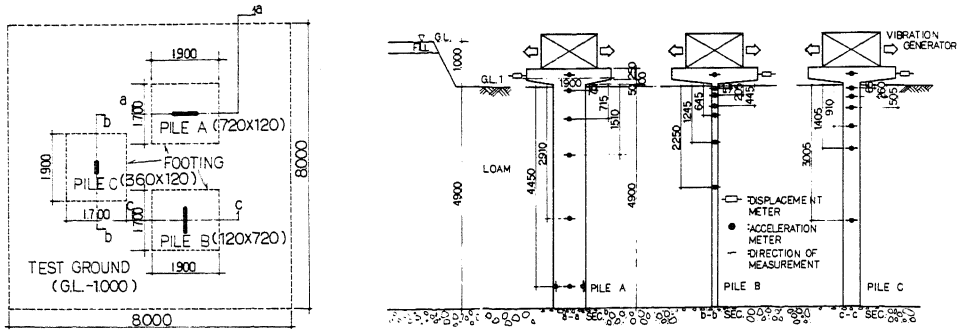

Fig. 1 Test Ground and Test Piles

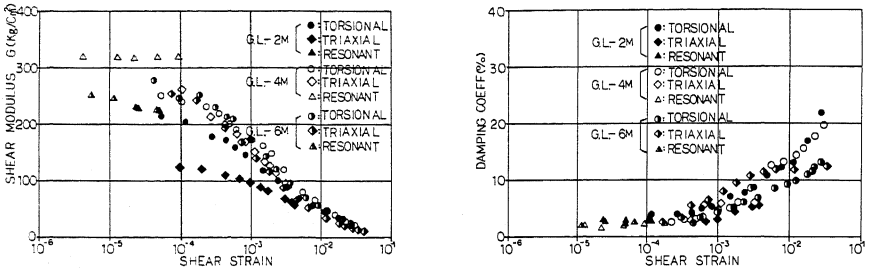

Fig. 2 Dynamic Properties of soil Samples

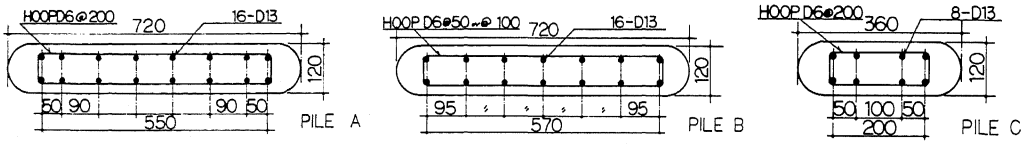

Fig. 3 Cross Section and Reinforcing Bar Arrangements of Test Piles

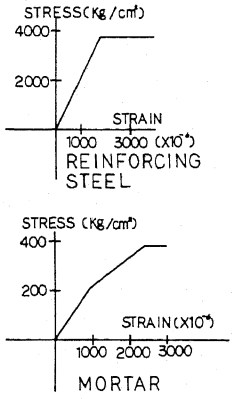

Fig. 4 Stress-Strain Relationship of Reinforcing Steel and Mortar

STEP-0	ER(ECCENTRIC MOMENT OF VIBRATION GENERATOR)=0.2kgm f1(1st. NATURAL FREQUENCY)=6.25Hz h(DAMPING COEFFICIENT)=5.1%
RUN-1	ER=2kgm M.A.F(MAXIMUM ACCELERATION OF FOOTING)=460gal M.D.F(MAXIMUM DISPLACEMENT OF FOOTIN)=0.3cm
STEP-1	ER=0.2kgm f1=5.8Hz h=4.7%
RUN-2	ER=6kgm M.A.F=680gal M.D.F=0.8cm
STEP-2	ER=0.2kgm f1=5.1Hz h=3.8%
RUN-3	ER=20kgm M.A.F=980gal M.D.F=2.5cm
STEP-3	ER=0.2kgm f1=3.0Hz h=6.3%

Tab. 1 Example of Experimentation Procedure

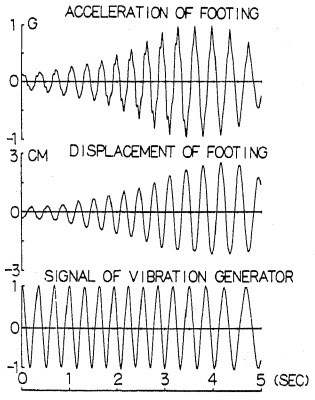

Fig. 5 Example of Recorded Waveform

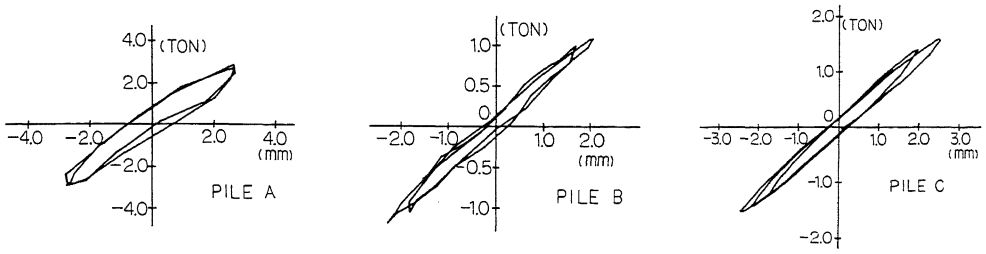

Fig. 6 Dynamic Hysteresis Loops (Small Deformation)

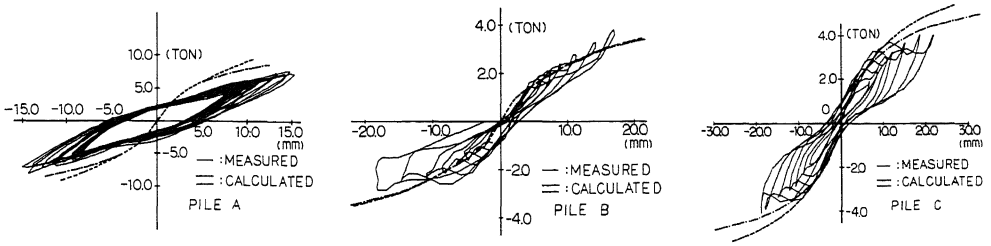

Fig. 7 Dynamic Hysteresis Loops (Massive Deformation)

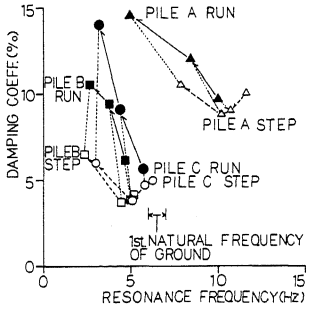

Fig. 8 Relationship between Damping Quantities and Resonance Frequencies

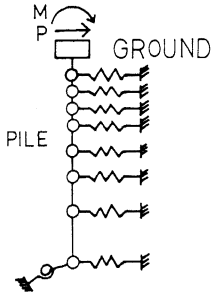

Fig. 9 Analytical Model of Soil-Pile System

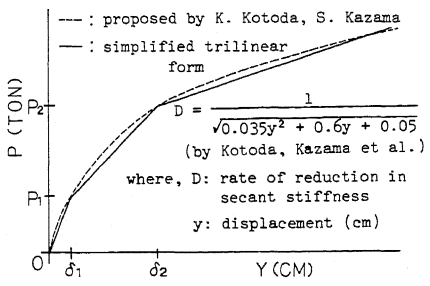

Fig. 10 Skelton Curve of Subgrade Reaction

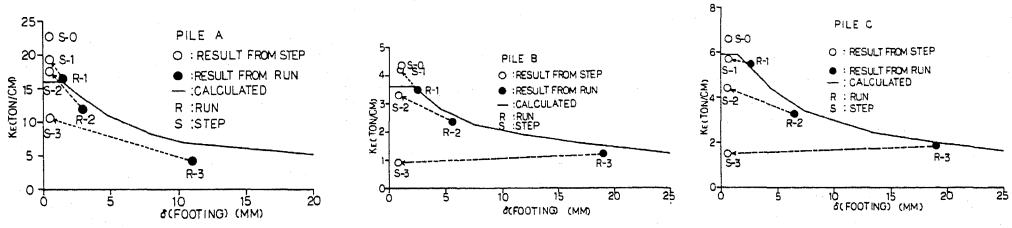

Fig. 11 Relation between Equivalent Stiffnesses and Footing Deformations

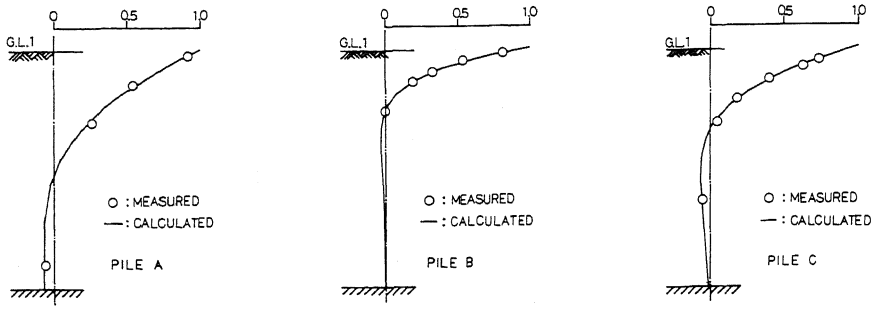

Fig. 12 Normalized Deformation Distributions of Piles

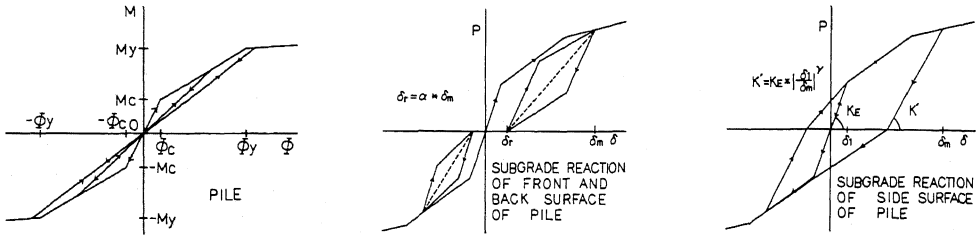

Fig. 13 Restoring Force Characteristics used in Analyses

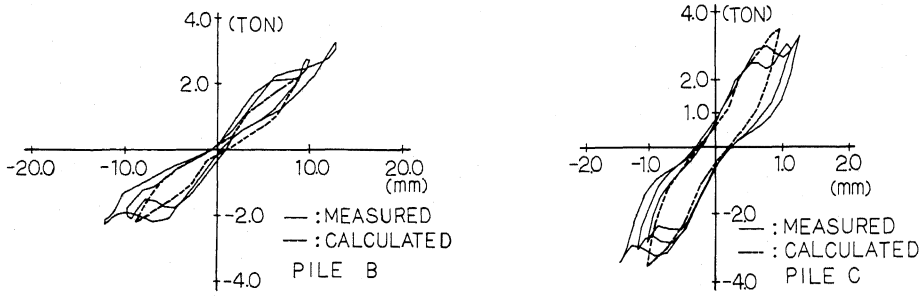

Fig. 14 Comparison between the Measured and Calculated Hysteresis Loop

REFERENCES

(Ref. 1) Novak, M., and Nogami, T., "Soil-Pile Interaction in Horizontal Vibration," Int. J. Earthq. Engrg. Struct. Dyn. 5, 263-281 (1977).

(Ref. 2) WFS Study Group, "A Study Regarding Dynamic Analysis of Structures Supported by Wall Foundation System," Proc. the 7th WCEE, 1980.

(Ref. 3) Kotoda, K., Kazame, S., et al., "Coefficient of Horizontal Subgrade Reaction (Part 7, Nonlinearity and Evaluation of K_H)," Proc. the 16th Annual Meeting, JSSMFE, pp 1421-1424 (in Japanese).